


Land use controls Kenyan riverine nitrate discharge into Lake Victoria – evidence from Nyando, Nzoia and Sondu Miriu river catchments

Benjamin Nyilitya, Stephen Mureithi & Pascal Boeckx

To cite this article: Benjamin Nyilitya, Stephen Mureithi & Pascal Boeckx (2020): Land use controls Kenyan riverine nitrate discharge into Lake Victoria – evidence from Nyando, Nzoia and Sondu Miriu river catchments, *Isotopes in Environmental and Health Studies*, DOI: [10.1080/10256016.2020.1724999](https://doi.org/10.1080/10256016.2020.1724999)

To link to this article: <https://doi.org/10.1080/10256016.2020.1724999>

 View supplementary material [↗](#)

 Published online: 18 Feb 2020.

 Submit your article to this journal [↗](#)

 Article views: 31

 View related articles [↗](#)

 View Crossmark data [↗](#)



Land use controls Kenyan riverine nitrate discharge into Lake Victoria – evidence from Nyando, Nzoia and Sondu Miriu river catchments^{*}

Benjamin Nyilyitya ^{a,b}, Stephen Mureithi^b and Pascal Boeckx ^a

^aIsotope Bioscience Laboratory - ISOFYS, Department of Green Chemistry and Technology, Faculty of Bioscience Engineering, Ghent University, Gent, Belgium; ^bDepartment of Land Resource Management and Agricultural Technology, University of Nairobi, Nairobi, Kenya

ABSTRACT

Nitrate (NO_3^-) sources and discharge were investigated using isotope and hydrochemical analyses in three river catchments draining Lake Victoria basin, Kenya. Hierarchical cluster analysis grouped Nyando, Nzoia and Sondu Miriu River stations into clusters corresponding to major land use classes of the catchments. Mixed agriculture (MA) in Nyando showed higher NO_3^- compared to the other land uses. Nitrate levels obtained ($0.1\text{--}11.6 \text{ mg L}^{-1}$) are higher than those reported in previous studies. Hydrochemistry support isotope data indicating that ammonium-based fertilizers and soil N were the major NO_3^- sources in tea dominated areas with average $\delta^{15}\text{N}$ ($6.5 \pm 1.3 \text{ ‰}$), $\delta^{18}\text{O}$ ($6.7 \pm 2.3 \text{ ‰}$) values. Manure/sewage were the main source in MA areas with average $\delta^{15}\text{N}$ ($8.4 \pm 2.4 \text{ ‰}$), $\delta^{18}\text{O}$ ($7.8 \pm 5.4 \text{ ‰}$) values. Sewage was the likely source in urban, residential & industrial areas recording average $\delta^{15}\text{N}$ ($10.0 \pm 2.4 \text{ ‰}$), $\delta^{18}\text{O}$ ($6.9 \pm 3.7 \text{ ‰}$) values. $\delta^{15}\text{N}$ between land uses were significantly different ($p < 0.0001$) while $\delta^{18}\text{O}$ were similar ($p = 0.4$). Seasonally, inorganic/organic fertilizers influenced river NO_3^- mostly in the wet cropping season. Lower NO_3^- concentrations observed in Nyando and Sondu Miriu during dry or start-wet season could be a result of *in situ* denitrification.

ARTICLE HISTORY

Received 29 August 2019
Accepted 14 December 2019

KEYWORDS


Denitrification; hydrochemistry; isotope hydrology; Kenya; nitrate pollution; nitrogen-15; Lake Victoria; land-use; oxygen-18

1. Introduction

Nitrate (NO_3^-) pollution of surface and groundwater resources has become a worldwide environmental problem threatening fresh water resources in many parts of the world [1]. High NO_3^- concentrations in aquatic environments can cause eutrophication, and at the same time pose health risks to humans such as methemoglobinemia in children (blue baby syndrome) and cancer following long term exposure [2]. Consequently, the World Health Organization has set a limit of 50 mg L^{-1} NO_3^- for drinking water, although recent findings by Schullehner et al. [3] report increased colorectal cancer risk at drinking water NO_3^- concentrations as low as 3.9 mg L^{-1} . Increasing input of NO_3^- into water bodies

CONTACT Benjamin Nyilyitya  Benjamin.nyilyitya@ugent.be or  kyalob73@yahoo.com

^{*}Originally presented at the IAEA Symposium on Isotope Hydrology 2019, Vienna, Austria, 20–24 May 2019.

 Supplemental data for this article can be accessed at <https://doi.org/10.1080/10256016.2020.1724999>

© 2020 Informa UK Limited, trading as Taylor & Francis Group

is attributed to intensive land use practices such as increased use of N-containing organic and inorganic fertilizers, industrial and urban discharges, and elevated atmospheric N deposition [4].

However, in the Lake Victoria, Africa's largest fresh water body (surface area: 68,000 km²) [5], a ca. 100-fold increasing trend in NO₃⁻ concentration has been reported over a period of ca. 50 years: studies done in 1965 [6] yielded 15–29 µg L⁻¹, in 1990 [7] 24.8 ± 21.8 µg L⁻¹, in 1998 [8] 66.6 ± 44.0 µg L⁻¹, in 2002 [9] 48.2 ± 21.4 µg L⁻¹, in 2009 [5] 98.7 ± 36.4 µg L⁻¹, and up to 990–2900 µg L⁻¹ in 2006 [10].

This has resulted in eutrophication of Lake Victoria with increasing levels of reactive nitrogen in water bodies [11] and in turn fuelled the rapid proliferation of water hyacinth (*Eichhornia crassipes*) and decrease in fish population [8]. This happens against the backdrop that the Lake is a great socio-economic resource of the East African Community partner states for fisheries, tourism, transport, water, and energy among others, and a core to East Africa regional integration and development.

The Kenyan catchment contributes around 40% of the surface water inflow of Lake Victoria and is estimated at about 292.1 m³ s⁻¹ [12]. The catchment is drained by several rivers, major ones being the Nyando River, Nzoia River and Sondu Miriu River. The rivers drain diverse land uses, ranging from pristine forests, commercial agricultural areas (tea, sugarcane, maize and horticulture), mixed smallholder agriculture with livestock farming, urban centres, industrialized towns and wetlands. The basin is subjected to both a high population growth rate (>6% p.a.) and fast urbanization, due to the economic importance of its fresh water resources for domestic, agricultural and industrial purposes. The population pressure and economic development have led to land use change in the basin, which has in turn negatively impacted ecosystems [13]. The basin, therefore, epitomizes a land degradation problem caused by deforestation, forest encroachment by smallholder farms, biomass burning (charcoal production) and poor land management practises. This has led to modification of physical, chemical and biological characteristics of rivers and as a consequence also Lake Victoria. This has been exemplified via remote sensing and demonstrated by an extending sediment plume in the Winam Gulf covering about 40 km² from the Nyando River mouth [14].

Therefore, given the environmental challenges and health risks posed by the uncontrolled discharge of NO₃⁻ into Lake Victoria, there is an important need to understand NO₃⁻ concentrations, sources and discharge by its tributary river catchments. Riverine nitrogen has been reported as the second most important source (after atmospheric deposition) of nitrogen loading into the lake, estimated at 16% [13,15]. Previous studies on this part of the Lake Victoria basin have focused on limnology and nutrient enrichment of the lake waters which has revealed an increasing NO₃⁻ concentration trend [8,9]. With the effects of eutrophication threatening the lake's ecosystem, recent emphasis has been on impact mitigation. As such, research and environmental management efforts in the basin have been focused on point NO₃⁻ sources like urban and industrial effluents as well as nutrient buffering and removal systems [16,17]. However, data on riverine NO₃⁻ discharge in Lake Victoria and other tropical lakes in Sub-Saharan Africa is scanty, and no study has attempted to investigate NO₃⁻ discharge and its sources from diverse land use of the major river catchments (Nyando, Nzoia, Sondu Miriu), draining the Kenyan part of the Lake Victoria basin.

The common approach in NO₃⁻ pollution management is monitoring concentrations in water with a comparison against threshold values, i.e. WHO limit of 50 mg L⁻¹. However,

this method does not provide information on sources of NO_3^- and limits dedicated mitigation strategies. Research has demonstrated added value of using dual isotopes of NO_3^- ($\delta^{15}\text{N}$ -, $\delta^{18}\text{O}$ - NO_3^-) to distinguish between sources of NO_3^- , which is based on the fact that potential sources such as inorganic fertilizers, sewage, manure, soil nitrogen and atmospheric deposition have distinct isotopic characteristics [2,18]. Moreover, studies have integrated $\delta^{15}\text{N}$ -, $\delta^{18}\text{O}$ - NO_3^- with hydrochemistry to study NO_3^- sources in large river basins; e.g. Yili river of the Taihu Lake watershed, China [19], Mississippi and Illinois river basins in the USA [20], and rivers draining watersheds in North-eastern USA [21]. As far as we are aware, this study is the first of its kind in tropical Africa, and integrates physicochemical data, hierarchical cluster analysis and isotope methods to quantify and understand NO_3^- discharge contribution from different land use areas to riverine NO_3^- . Specifically, this study provides (1) information on potential NO_3^- sources (based on hydrochemistry, $\delta^{15}\text{N}$ - and $\delta^{18}\text{O}$ - NO_3^- data), and (2) baseline hydro-chemical data of Kenyan rivers draining into Lake Victoria. It is hypothesized that land use intensity has a dominant effect on river NO_3^- concentrations and sources. All together, our findings can contribute to start establishing dedicated management plans for NO_3^- discharge mitigation in the basin.

2. Materials and methods

2.1. Study area

The study was conducted in three river catchments: Nyando, Nzoia and Sondu Miriu draining the Kenyan side of Lake Victoria (Figure 1). River Nyando (Supplementary file: Figure

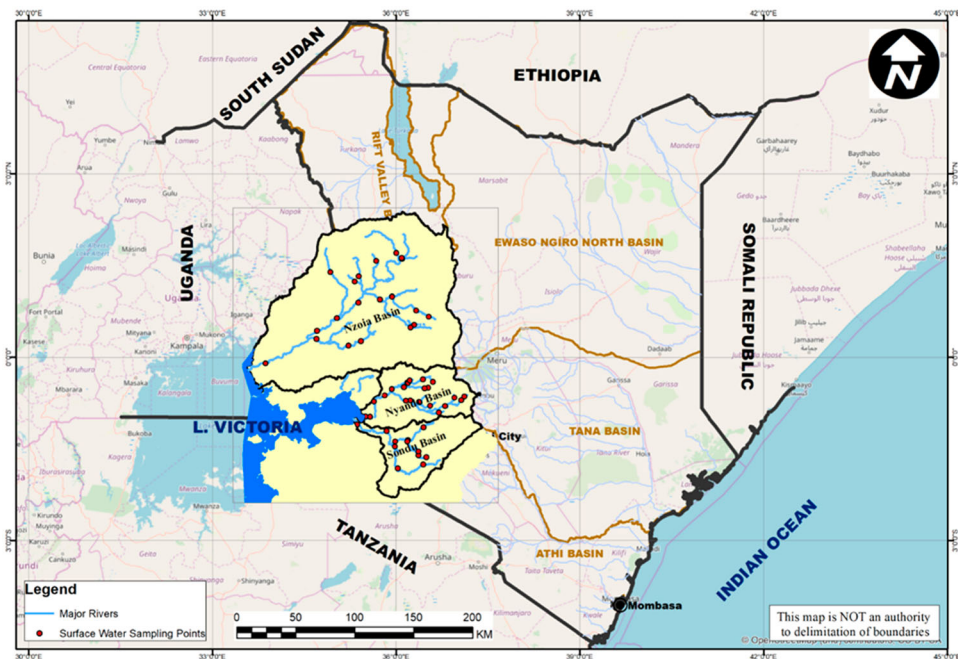


Figure 1. Map of Kenya in East Africa with inset: study area with major rivers (Nyando, Nzoia, and Sondu Miriu) and sample points (dots). The equator (latitude 0°) pass through the study area.

1a) is 153 km long and originates from western Mau and Nandi hills. It drains a catchment area of 3,590 km², has an average discharge rate of 18 m³ s⁻¹ and drains into the Winam Gulf of Lake Victoria [12]. Key land use patterns in the Nyando catchment include the pristine Mau forests, commercial tea, sugarcane, horticultural flower farms, mixed agriculture, mushrooming urban centres, industries and wetlands at the river mouth. River Nzoia (Supplementary file: Figure 1b), on the other hand, is the largest one of the three rivers. It originates from Cherengani hills with tributaries from Mt. Elgon and drains a catchment area of 12,709 km². Having a length of 334 km and an average discharge rate of 115.3 m³ s⁻¹, the River Nzoia provides the second largest tributary flow to Lake Victoria after the River Kagera from Rwanda [12]. River Nzoia drainage network consists of diverse land uses including mixed agriculture in the upstream catchments, major urban centres, commercial sugarcane, maize and wheat farming and agro-based industries. River Sondu Miriu (Supplementary file: Figure 1c) has its headwaters in the south-western block of the Mau complex, drains a catchment area of 5,180 km² with an average discharge rate of 42.2 m³ s⁻¹ [12] and drains into the Winam Gulf of Lake Victoria. River Sondu Miriu drainage area consists of natural forests at the headwater catchment. Planted forests and commercial tea estates occupy the midstream, while mixed agriculture and a hydroelectric power generation plant are the major land use in the downstream before its entry into Lake Victoria.

The study area experiences a long rain season between March and July and a short rainy season between September and November. However, during the study period, the area got erratic rainfall pattern compared to the long-term pattern (Figure 2). Unusually low rainfall appeared in the months of October and December, and a general temperature increase (>0.5°C) was observed comparing the sampling period to the long-term data. These weather anomalies may be associated to the impacts of global warming which is not only limited to changes in temperature but also alters rainfall amount, distribution and pattern [22].

2.2. Sampling and analysis

Selection of field sampling stations was done in consultation with the Lake Victoria Basin Commission's Environmental Management Project and the Water Resources Authority who run the Lake Victoria basin water quality-monitoring network. Spatial sampling stations in the Nyando catchment were identified and located right from the headwater catchment consisting of pristine forest and commercial tea estate, commercial sugarcane estates, horticultural farm, mixed agriculture (which according to this study refers to: smallholder agriculture ca. < 5 ha and livestock keeping), industrial and urban centres, wetland and river mouth. In the more expansive Nzoia catchment, stations were spatially distributed across the main channel, first and second order streams covering commercial sugarcane farms and sugar factories, large maize and wheat farms (ca. ≥ 5 ha), mixed agriculture, urban and industrial centres. In the Sondu Miriu catchment where tea farming is the major agricultural activity, stations were spatially spread covering mixed agriculture (maize, beans, sorghum, livestock) at lower reaches, tea growing (commercial and smallholder) at the midstream to upstream zone, and the urbanized Kericho town area.

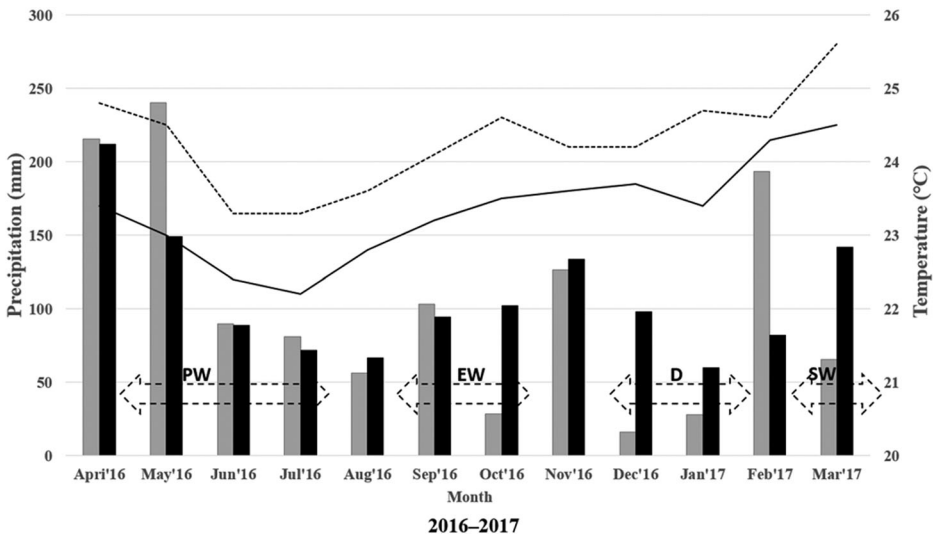


Figure 2. Monthly average rainfall and temperature registered at the Ahero (Kisumu) weather station. Long term (1967–1994) and study period (2016–2017) data are given for precipitation 2016–2017 (grey bars), precipitation 1967–1994 (black bars), temperature 2016–2017 (dotted line), and temperature 1967–1994 (full line); sampling periods include: peak wet cropping season (PW), end of wet season (EW), dry season (D), start of wet season (SW); Source: Kenya Meteorological Department.

A spatiotemporal sampling strategy was carried out at 22 sampling stations along the River Nyando, 21 stations in the River Nzoia catchment, and 13 stations along the River Sondu Miriu. To capture seasonal variation in NO_3^- discharge, grab sampling was carried out in four seasons: (1) during an agricultural productive, wet period from May to July 2016, marked as ‘peak wet’ season, (2) during the ‘end of the wet’ season in September 2016, (3) during the ‘dry season’ in December 2016, and (4) at the transition period from dry to wet season in March 2017, marked as ‘start of wet’ season (Figure 2).

In the field, water was taken as a grab sample in 200 mL high density polyethylene bottles, pre-filtered onsite (11 μm Whatmann filters) and stored in an insulated cooler box containing ice cubes for transportation to the laboratory for physicochemical and isotope analysis. Duplicate samples for cation analysis were taken in 100 mL HDPE bottles, pre-filtered and acidified to pH 2 using dilute nitric acid. *In situ* measurements included temperature (T), electrical conductivity (EC), pH, dissolved oxygen (DO) and discharge measurements of river water. These *in situ* parameters (T, EC, pH, DO) were measured at every sampling station using a multi-parameter sensor (2FD47F-Multi3430, WTW, Germany). Discharge measurements were carried out using a universal current flow metre (F1, Hydrokit, Germany) at the last sampling station before river mouth to estimate NO_3^- discharge of the river catchments into Lake Victoria. In the laboratory, all samples were filtered through 0.45 μm membrane filters and stored frozen (-17°C) awaiting analysis. Laboratory determination of Na^+ , K^+ , Ca^{2+} , Mg^{2+} , NH_4^+ , NO_3^- , Cl^- , SO_4^{2-} and PO_4^{3-} concentrations was carried out using an ion chromatograph (930 Compact IC Flex, Metrohm, Switzerland). The $\delta^{15}\text{N}$ - and $\delta^{18}\text{O}$ - NO_3^- values were determined by the ‘Bacterial denitrification method’ [18,23,24], which allows for simultaneous determination of $\delta^{15}\text{N}$

and $\delta^{18}\text{O}$ of N_2O produced from the conversion of NO_3^- by denitrifying bacteria, which naturally lack N_2O -reductase activity. The $\delta^{15}\text{N}$ and $\delta^{18}\text{O}$ analyses of the produced N_2O were carried out using a trace gas preparation unit (ANCA TGII, SerCon, UK), coupled to an isotope ratio mass spectrometer (IRMS) (20–20, SerCon, UK). The N_2O sample was flushed out of the sample vial using a double-hole needle on an auto-sampler. Water was removed using a combination of nafion dryer and $\text{Mg}(\text{ClO}_4)_2$ scrubber. By cryogenic trapping and focusing, the N_2O was compressed onto a capillary column (CP-Poraplot Q 25, 0.32 mm id, 10 μm df, Varian, US) at 35°C and subsequently analysed by IRMS. The subsequent stable isotope data were expressed as delta (δ) units in per mil (‰) notation relative to the respective international standards:

$$\delta_{\text{sample}} (\text{‰}) = \left[\frac{R_{\text{sample}}}{R_{\text{standard}}} - 1 \right] \times 1000 \quad (1)$$

where R_{sample} and R_{standard} are the $^{15}\text{N}/^{14}\text{N}$ or $^{18}\text{O}/^{16}\text{O}$ ratio of the sample and the standard for $\delta^{15}\text{N}$ and $\delta^{18}\text{O}$, respectively. The $\delta^{15}\text{N}$ values are reported relative to N_2 in atmospheric air (AIR) and $\delta^{18}\text{O}$ are reported relative to Vienna Standard Mean Ocean Water (VSMOW). Three internationally recognized reference standards, USGS32 ($180.0 \pm 1.0 \text{‰}$ for $\delta^{15}\text{N}$, $25.7 \pm 0.4 \text{‰}$ for $\delta^{18}\text{O}$), USGS34 ($-1.8 \pm 0.2 \text{‰}$ for $\delta^{15}\text{N}$, $-27.8 \pm 0.4 \text{‰}$ for $\delta^{18}\text{O}$), and USGS35 ($2.7 \pm 0.2 \text{‰}$ for $\delta^{15}\text{N}$, $56.8 \pm 0.3 \text{‰}$ for $\delta^{18}\text{O}$), were used to normalize the raw $\delta^{15}\text{N}$ and $\delta^{18}\text{O}$ values (based on a N_2O reference gas tank) to the AIR and VSMOW scale. USGS32 and USGS34 were used for normalization of the $\delta^{15}\text{N}$ value, and USGS34 and USGS35 for the $\delta^{18}\text{O}$. The amount of NO_3^- in samples and references were matched (i.e. 20 nmol) which corrects for nonlinearity of the IRMS and blanks associated with the procedure. An in-house KNO_3 laboratory standard (9.9‰ for $\delta^{15}\text{N}$, 24.3‰ for $\delta^{18}\text{O}$), was analysed together with the samples for quality control. Measurement batches were only accepted if measured $\delta^{15}\text{N}$ and $\delta^{18}\text{O}$ values of the laboratory standard were within 0.4 and 0.5 ‰ of our accepted values, respectively. If standard deviation on replicate samples was higher than 0.3 and 0.4 ‰ for $\delta^{15}\text{N}$ and $\delta^{18}\text{O}$, respectively, the sample was reanalyzed. More details are provided in Casciotti et al. [23], and Xue et al. [18]. In order to determine the denitrification potential in the riverbeds, a laboratory experiment using superficial riverbed sediments from the study area was set up as described by Dhondt et al. [25]. 20 g of dried and sieved (2 mm) riverbed sediments were weighed into a 500 ml Schott bottle. 300 ml of water solution (MQ water containing 20 μM CaCl_2) was added and the bottles sealed with bottle caps containing two holes fitted with pipes to flush the bottle (both sediment and airspace) using N_2 gas to remove O_2 from the system. After 2 days of anaerobic pre-incubation, Nitrapyrin was added as nitrification inhibitor at a concentration of 120 mg kg^{-1} dry soil. In the current study, no external carbon source was added other than the natural organic carbon of the sediments. Therefore, NO_3^- was added to the solution based on the sediment carbon content to ensure an electron donor/electron acceptor ratio, which promotes denitrification in the system. Samples of the soil suspension were abstracted with a syringe at regular time intervals (0, 4, 8, 24, 30 and 48 hours) and analysed for NO_3^- . The sediment samples, which showed NO_3^- reduction with time, were further analysed for $\delta^{15}\text{N}$ and $\delta^{18}\text{O}$ to demonstrate that NO_3^- reduction can potentially occur in the riverbeds thereby biasing isotopic

signature of NO_3^- . This relationship is expressed by a Rayleigh equation:

$$\delta_s = \delta_0 + \varepsilon \ln(f) \quad (2)$$

where δ_0 is the initial $\delta^{15}\text{N}-\text{NO}_3^-$ value, δ_s is the $\delta^{15}\text{N}-\text{NO}_3^-$ value in the remaining NO_3^- , f is the fraction of the remaining NO_3^- and ε is the isotope enrichment factor.

2.3. Statistics

Water physicochemical dataset of spatial sampling stations was analysed using hierarchical cluster analysis (HCA). The data for HCA (agglomeration schedule) analysis was first standardized by subtracting the mean value and dividing by the standard deviation of the parameter in order to eliminate the influence of different units between variables. HCA was performed on the data sets (using the following variables: Na^+ , K^+ , Ca^{2+} , Mg^{2+} , NO_3^- , Cl^- , SO_4^{2-} , pH, EC, T and DO) by means of the Ward's method using squared Euclidean distances as a measure of similarity in order to cluster sampling stations into homogeneous groups. The results were presented in a dendrogram showing the clusters and their proximity with a reduction in the dimensionality of the original data set. HCA has been applied in the past for surface and groundwater quality assessment and land use segmentation [26–29]. ANOVA with Tukey HSD tests ($p < 0.05$ levels) were performed on the NO_3^- , $\delta^{15}\text{N}$ and $\delta^{18}\text{O}$ data to understand interactions between different land uses.

Major ionic constituents were plotted in piper (1944) tri-linear diagrams [30]. These are a combination of anion and cation triangles with a diamond shape between them which plots the analysis, and whose position indicates the water type or water origin. Using the AquaChem (version 2014.2) software package, water types helped in understanding the processes controlling river water mineralization, which by extension indicates NO_3^- origin. In addition, NO_3^- versus Cl^- correlations were plotted to establish probable pathways controlling NO_3^- input in the river water [31].

3. Results and discussion

3.1. Spatial clustering of sampling stations

River physicochemical data from a spatiotemporal sampling campaign in Nyando, Nzoia, and Sondu Miriu river catchments were analysed using HCA, which grouped sampling stations with similar properties together. Figure 3a-c gives HCA output dendrograms grouping sampling stations for the Nyando catchment into four clusters, and for the Nzoia catchment and Sondu Miriu catchment into three clusters. The clusters, which in comparison to land use maps (Supplementary file: Figure 1a–c) correspond to the major land use classes in the three river catchments informed the allocation of sample point identities (i.e. MA, S, T, CA ...).

For the Nyando catchment (Figures 3a), HCA grouped stations in the upper reaches of the Kipchorian tributary into cluster 1. The area lies at 1900–2300 m a.s.l. and features mixed agriculture (MA) areas under food crop cultivation, a commercial horticultural flower farm, livestock keeping, and residential settlements. MA1, MA2, MA4 and MA5 are situated in an intensive agriculture and peri-urban area, while MA3 is located

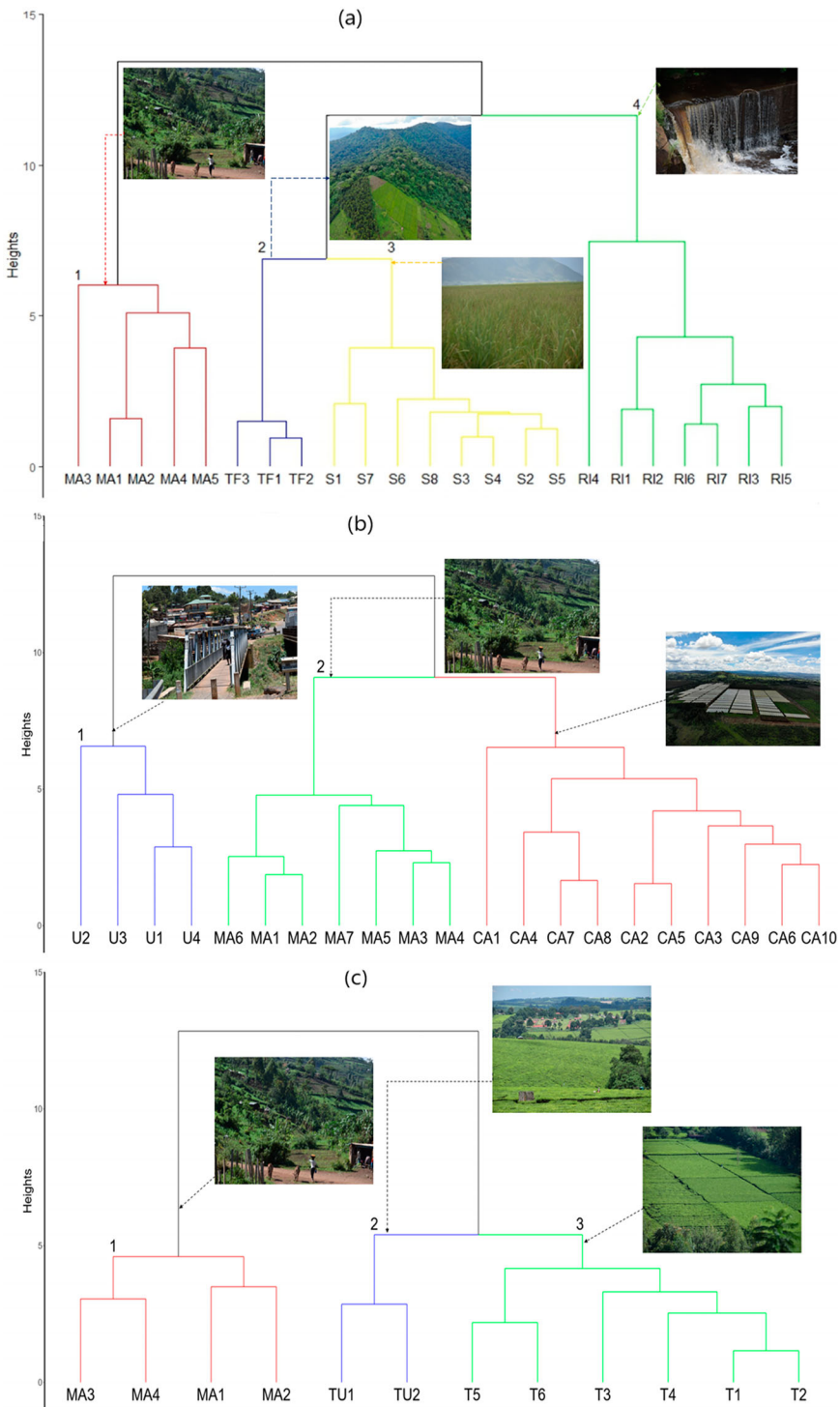


Figure 3. HCA cluster dendrograms (Ward’s method, squared Euclidean distance) grouping sampling stations in the Nyando (a), Nzoia (b) and Sondu Miriu (c) river catchments; clusters are labelled by dominant land use i.e. MA: mixed agriculture, TF: tea and forests, S: sugarcane, RI: residential settlements and industrial, CA: commercial agriculture, U: urban, TU: tea and urban, T: tea.

downstream of the commercial horticultural flower farm. Cluster 2 groups stations under tea and forest (TF1–TF3) located at the most upstream part of the catchment. TF1 is located in a pristine forest, which is part of the Mau complex, while TF2 is located in a commercial tea estate and TF3 in an area of smallholder mixed farms bordering the natural forest. Cluster 3 groups sample stations within the sugarcane belt (S1–S8) downstream of the tea area and forest. As can be observed from the HCA dendrogram, cluster 2 and cluster 3 areas have similar physicochemical properties and form one major group representing the river Ainapngetuny (Supplementary file: Figure 1a), one of the two main tributaries of River Nyando. Cluster 4 stations represent residential and industrial areas (R1–R17); they are located in the mid- to downstream reaches of the Nyando catchment. The area is characterized by relatively high-populated residential and urban centres, agro-based industries (sugar, agrochemical, and lime factory), rice irrigation and affected wetlands.

For the Nzoia catchment (Figure 3b), HCA grouped stations located in major urban centres like Eldoret and Moi's bridge towns into cluster 1 (U1–U4). These areas feature sewage effluent discharges consisting of industrial and domestic waste. Cluster 2 consists of stations located in second and third order streams found in the upper reaches of the catchment whose common land use is mixed agriculture (MA) on small land parcels measuring ≤ 2 ha. Cluster 2 stations were also characterized by land degradation practices like deforestation and farming on steep slopes and un-terraced lands, which leads to high soil erosion rates. Cluster 3 groups stations mainly under commercial agriculture (CA) of sugarcane, maize and/or wheat. Farms in cluster 3 consist of large-scale mechanized farms owned by state corporations like Nzoia and Mumias sugar companies, which run sugarcane milling, ethanol and molasses production factories. In addition, the area has small-scale farmers who have ventured into cash crops (sugarcane, wheat, maize) for commercial purposes. Furthermore, cluster 3 stations are located in the main Nzoia catchment and its first order streams.

For the Sondu Miriu catchment (Figure 3c), HCA groups stations in mixed agriculture (MA) areas located in the downstream part of the main river (MA1, MA2) and the lower reaches of the first order Kipsonoi tributary (MA3, MA4) into cluster 1. In this area, mixed agriculture (tea, maize, beans, sugarcane and sorghum), a hydropower dam, residential areas and livestock farming are the major land uses. HCA groups stations in the Ainapkoii tributary, which drains a purely commercial tea area and the urbanized Kericho town into cluster 2 (TU). Cluster 3 consists of stations (T1–T6) in a predominantly tea growing area of the Chemosit basin. The area is characterized by small-scale tea farms, commercial tea farms and planted forests. As observed in Figure 3c, cluster 2 and 3 stations form one main group (tea area), distinct in physico-chemistry from the mixed agricultural area.

3.2. Physicochemical and isotopic characterization

3.2.1. In-situ parameters

Table 1 presents a summary of *in situ* parameters obtained from the study area. Water EC values obtained in this study are within WHO standards for fresh water ($< 500 \mu\text{S cm}^{-1}$) ranging from a mean of $45 \mu\text{S cm}^{-1}$ in the tea land use of the Sondu Miriu catchment to $311 \mu\text{S cm}^{-1}$ in residential and industrial land use of the Nyando catchment. Moreover,

Table 1. Summary of *in situ* parameters: pH, electrical conductivity (EC), temperature (Temp), dissolved oxygen (DO) per land use clusters (see Figure 3 for explanation) in the three river catchments; river water and nitrate discharge values represents the last sampling point (before river mouth) for the Start wet (SW), Peak wet (PW), End wet (EW) and Dry (D) seasons.

River	Location	pH	EC ($\mu\text{S cm}^{-1}$)	Temp ($^{\circ}\text{C}$)	DO ($\text{mg O}_2 \text{ L}^{-1}$)	River water ($\text{m}^3 \text{ s}^{-1}$) and nitrate (t day^{-1}) discharge			
						SW	PW	EW	D
Nyando	S	8.3 ± 0.2	296 ± 47	22 ± 2	7.6 ± 0.3	4.0 ^a	37.4	8.7	3.0
	TF	7.9 ± 0.2	168 ± 27	17 ± 2	7.6 ± 0.2				
	MA	7.2 ± 0.9	184 ± 52	18 ± 3	7.0 ± 0.6	0.8 ^b	6.2	1.5	0.06
	RI	8.1 ± 0.3	311 ± 104	24 ± 2	6.4 ± 1.8				
Nzoia	CA	7.6 ± 0.3	123 ± 29	22 ± 2	7.4 ± 0.6	41 ^a	187	149	26.6
	MA	7.3 ± 0.3	90 ± 21	18 ± 2	7.3 ± 0.6	17.7 ^b	22.2	33.5	5.2
	U	7.7 ± 0.4	190 ± 55	20 ± 3	7.4 ± 0.4				
Sondur Miriu	T	7.1 ± 0.3	45 ± 9	18 ± 2	7.9 ± 0.3	6.1 ^a	22.9	16.2	8.9
	TU	6.9 ± 0.2	54 ± 7	18 ± 2	7.6 ± 0.2	2.3 ^b	7.2	5.3	2.6
	MA	7.4 ± 0.4	71 ± 19	22 ± 2	7.6 ± 0.4				

^aRiver water discharge.

^bNitrate discharge.

the Nyando catchment portrayed higher EC values than the other two catchments. A neutral to slightly alkaline water pH (mean pH 6.9– 8.3) was observed while DO values ($6.4\text{--}7.9 \text{ mg O}_2 \text{ L}^{-1}$) were sufficiently high for surface water and likely unfavourable for *in situ* denitrification processes [32,33] (see further). Water temperature in the study area was influenced by altitude with the lowest mean water temperature of 17°C recorded in the tea and forest (altitude: 1900–2200 m a.s.l), while the highest mean water temperature of 24°C was observed in the residential and industrial located near shores of Lake Victoria (altitude: 1140–1300 m a.s.l). The Nzoia catchment had the highest water discharge volumes during the study period, ranging $26 \text{ m}^3 \text{ s}^{-1}$ in the D season to $187 \text{ m}^3 \text{ s}^{-1}$ during the PW season. The River Sondur Miriu discharged from $6.1\text{--}22.9 \text{ m}^3 \text{ s}^{-1}$ while the Nyando ranged from 3 to $37.4 \text{ m}^3 \text{ s}^{-1}$. River nitrate discharge into the Lake Victoria were approximated from the river water discharge and NO_3^- concentration values (supplementary file: Table1–3) at the last sampling station before the river mouth (Figure 1). River Nzoia led in NO_3^- discharge into the Lake Victoria during the sampling period with a discharge between 5.2 and 33.5 t d^{-1} , respectively. Sondur Miriu ranked second discharging between 2.3 and 7.2 t d^{-1} while the Nyando discharged between 0.06 and 6.2 t d^{-1} . A study by Okungu and Opango [34], also reported the Nzoia catchment as leading source of total annual nutrient loading of Lake Victoria from the Kenyan side of the basin.

3.2.2. Nyando catchment

In order to characterize the river hydrochemistry under the different HCA determined land use areas of the Nyando catchment, major ions (Na^+ , K^+ , Ca^{2+} , Mg^{2+} , NO_3^- , HCO_3^- , Cl^- , SO_4^{2-}) were plotted in piper diagrams [30] and presented in Figure 4a. A clear spatiotemporal variation in ionic constituents was observed in the Nyando catchment, which also indicates the dominant solutes and water types in this catchment. In the MA stations, dominance of alkali metals (Na^+ , K^+) over alkaline earth metals (Ca^{2+} , Mg^{2+}) was found, while $\text{Cl}^- + \text{NO}_3^-$ were the major anions giving a Na + K-Cl + NO_3^- water type. Local geology normally influences dissolved river solutes and mainly reflected by base flow concentrations. However, the dominance of a Na + K-Cl + NO_3^- water type in MA in all seasons suggests

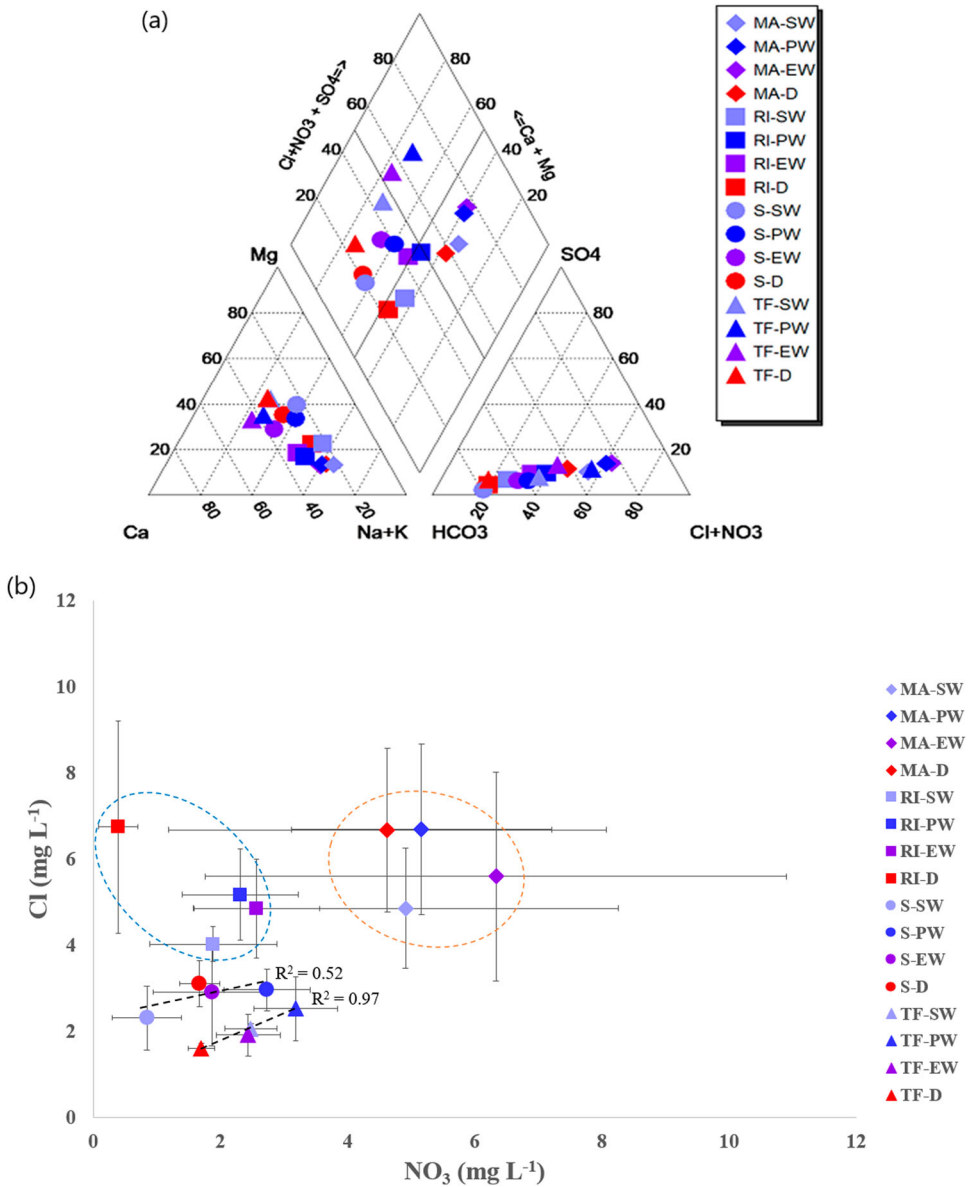


Figure 4. Nyando catchment: Piper trilinear plot of major cations and anions (in percent) for water characterization. Bullets represent land use clusters (see Figure 3 for abbreviations), while colours represent selected sampling seasons (see Figure 2 for abbreviations) (a); spatial temporal plot of mean Cl⁻ versus NO₃⁻ mean concentrations with standard deviations given as error bars and bullets represent land use clusters while colours represent seasons as described in (a) above (b); Ranges of NO₃⁻ concentration, $\delta^{15}\text{N}-\text{NO}_3^-$ and $\delta^{18}\text{O}-\text{NO}_3^-$ values obtained for different land use clusters in Nyando during start of wet (SW), peak wet (PW), end of wet (EW) and dry (D) seasons. Boxplots represent 25th, 50th, and 75th percentiles, whiskers represent 5th and 95th percentiles, black bullets represent outliers, and grey bullets represent mean values. Letters (a, b, c) represent ANOVA output with similar letters indicating non-significant difference ($p > 0.05$) using Tukey HSD test (c).

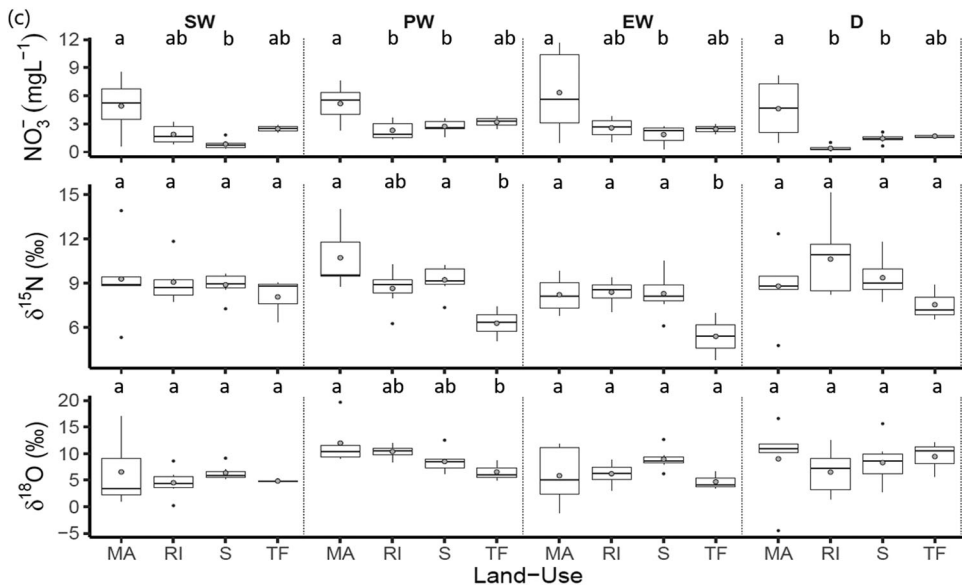


Figure 4 Continued

surface water contamination [27]. In TF, alkaline earth metals dominate over the alkali metals, while $\text{Cl}^- + \text{NO}_3^-$ and HCO_3^- are the major anions. In the diamond, TF plots in the $\text{Ca} + \text{Mg} - \text{HCO}_3^-$ and $\text{Ca} + \text{Mg} - \text{Cl} + \text{NO}_3^-$ water type during the dry and wet seasons, respectively. A $\text{Ca} + \text{Mg} - \text{HCO}_3^-$ water type represents soil weathering (natural) sources [35] implying that the $\text{Ca} + \text{Mg} - \text{Cl} + \text{NO}_3^-$ water type observed in TF during wet seasons reveals influence by inorganic fertilizers applied in tea. Similar to TF, S shows a $\text{Ca} + \text{Mg} - \text{HCO}_3^-$ water type with an increase in $\text{Cl}^- + \text{NO}_3^-$ during the wet seasons. RI seems to have both alkali (Na^+ , K^+) and alkaline earth (Ca^{2+} , Mg^{2+}) metals in similar proportions. HCO_3^- is the major anion in RI but an increase of $\text{Cl}^- + \text{NO}_3^-$ is again observed in the wet (PW, EW) seasons. The RI plots in the $\text{Na} + \text{K} - \text{HCO}_3^-$ water type during the dry seasons and shows both $\text{Ca} + \text{Mg} - \text{HCO}_3^-$ and $\text{Na} + \text{K} - \text{Cl} + \text{NO}_3^-$ water types during the wet seasons. The $\text{Cl}^- + \text{NO}_3^-$ increase observed in Nyando catchment during wet seasons is likely related to agricultural inputs (inorganic/organic fertilizer) which are mainly applied during the wet cropping season in commercial tea, sugarcane, horticultural and mixed farming [36]. The common fertilizer types used in the region are: NH_4^+ based NPK commonly applied in tea plantations; CAN and DAP commonly used in maize, wheat and beans; urea applied in sugarcane farming; $(\text{NH}_4)_2\text{SO}_4$ in rice farming; and animal manure commonly broadcasted in mixed farming systems for subsistence (e.g. maize, beans, sorghum, millet).

Chlorine behaves as a conservative ion in water whose concentration is not subject to physical, chemical and microbiological processes occurring within the river system and therefore a good indicator of anthropogenic impacts [37]. Potential sources of Cl^- include natural sources (mineral dissolution), inorganic fertilizers (KCl), animal wastes and sewage effluents. The NO_3^- vs. Cl^- correlations can provide more information on NO_3^- sources, and help to identify removal processes via denitrification [31,38]. Figure 4b shows a plot of Cl^- versus NO_3^- in the Nyando catchment in which samples cluster into three groups. TF and S stations cluster closely together in a group which shows linear

relationship ($R^2 = 0.97$, $R^2 = 0.52$ respectively) between Cl^- and NO_3^- pointing towards a contaminant source which causes a proportional Cl^- and NO_3^- increase from the dry to the peak wet season. The common source of Cl^- and NO_3^- should be the NPK fertilizer whose primary source of potassium is potash (KCl). NPK is applied during the peak wet cropping season in the commercial tea and sugarcane farms. Furthermore, there was a clear separation of MA land use stations into a group with high Cl^- and NO_3^- . The MA land use features high population density living in an urbanizing area lacking effluent treatment infrastructure and practicing mixed farming of food crops and free-range livestock keeping. The area also has a commercial horticultural flower farm under irrigation. Both manure and inorganic fertilizers (NPK, CAN, DAP) are used in the area at a rate ranging between 25 and 75 kg N ha⁻¹ yr⁻¹ for planting and top dressing. This therefore, indicates that inorganic fertilizer losses, animal wastes and sewage discharges are major sources of the Cl^- and NO_3^- in MA. RI stations, on the other hand, were separated in a group with high Cl^- but low NO_3^- concentration. RI is located in the downstream part of the Nyando catchment (Supplementary file: Figure 1a), which together with being a residential and relatively industrialized area, also has an irrigated rice farming zone and an extensive wetland towards the river mouth. As shown in Figure 4b, there seems a mechanism in RI, which selectively consumes NO_3^- without affecting the Cl^- concentration.

In spite of the high DO values (which do not favour denitrification) obtained in RI (Table 1), denitrification in riparian zones has been reported to reduce NO_3^- load of stream water [39]. As NO_3^- concentration decreases, denitrification causes an enrichment of $\delta^{15}\text{N}$ -, $\delta^{18}\text{O}$ - NO_3^- while NO_3^- concentration decreases in the remaining NO_3^- pool [38]. Denitrification is illustrated by the enriched $\delta^{15}\text{N}$ - NO_3^- values ranging from +8.2 to +15.1 ‰ observed in RI in the dry season corresponding to significantly low NO_3^- concentration ranging from 0.1 – 1.0 mg L⁻¹ (Figure 4c and Supplementary file: Table 1). For instance, RI.3 RI.6 and RI.7 recorded very low NO_3^- values during the dry season: 0.2, 0.3 and 0.2 mg L⁻¹ respectively corresponding to $\delta^{15}\text{N}$ - NO_3^- of 8.3, 11.1 and 8.6 ‰, respectively, which can be attributed to denitrification in the rice fields and the river mouth wetland. Furthermore, the average NO_3^- concentration in RI in the dry season (0.4 ± 0.1 mg L⁻¹) was significantly lower compared to the other land uses ($p = 0.03$) and seasons ($p < 0.0001$). On the other hand, the corresponding average $\delta^{15}\text{N}$ - NO_3^- (10.6 ± 6.3 ‰) was higher than average values obtained in the other land uses ($p = 0.09$) and seasons ($p = 0.009$).

MA land use recorded higher NO_3^- concentrations compared to the other land use clusters during the sampling period (Figure 4c). The highest NO_3^- concentration (5.6 – 11.6 mg L⁻¹) were obtained in MA3, which drains a commercial horticultural flower farm. $\delta^{15}\text{N}$ - NO_3^- for MA points ranging from +4.8 to +14 ‰ portray the dominance of manure and/or sewage NO_3^- source and was more pronounced (+9.5 to +14 ‰) in the PW cropping season mainly due to animal manure application in the mixed farms. Nonetheless, $\delta^{18}\text{O}$ - NO_3^- values obtained in MA3: 17.0 (SW), 19.6 (PW), and 16.6 ‰ (D) lie in the nitrate fertilizer source range, +17 to +25 ‰ [18] and shows that inorganic fertilizers used in the irrigated commercial flower farm has impact on river water NO_3^- input in the MA land use. On the other hand, relatively low $\delta^{15}\text{N}$ - NO_3^- values ranging from +3 to +7 ‰ which were obtained in TF during PW and EW seasons lie in the literature range for both soil N and ammonium-based fertilizer sources [2]. However, the lower $\delta^{18}\text{O}$ - NO_3^- observed in this land use during the wet season supports the inorganic fertilizer contribution assuming that the $\delta^{18}\text{O}$ - NO_3^- in rainfall is constant across all land uses during

the wet season. In the TF, the ammonium-based fertilizer: NPK (25:5:5 + 5S) is most commonly used during wet seasons (PW, EW) for soil fertility improvement. It therefore suggests that, during the drier (D, SW) seasons, the $\delta^{15}\text{N}\text{-NO}_3^-$ (+6.4 – +9.0 ‰) and $\delta^{18}\text{O}\text{-NO}_3^-$ (+4.7 – +12.0 ‰) values obtained in the TF area originate from leaching of mineralized soil organic N in the dense natural forest. The isotope data supports the hydro-chemical observations (Figure 4a and b) thereby confirming that inorganic fertilizer loss in TF dominate river NO_3^- in the wet seasons while manure and sewage plus inorganic fertilizer (commercial horticulture) control river NO_3^- input in MA. The results also show the leading influence of manure and sewage (urban, industrial) on river NO_3^- in the RI while inorganic fertilizers influence river NO_3^- in the S land use during the wet season.

However, *in situ* nitrate removal processes could be responsible for low NO_3^- values obtained in different parts of the catchment. Just as observed in RI stations, significantly low NO_3^- contents (0.4 – 1.8 mg L⁻¹) were recorded in S land use during SW season which were below the natural forest value (background estimate: 2.9 mg L⁻¹) (Figure 4c). Since this selective NO_3^- reduction in downstream Nyando (S, RI) cannot be caused by dilution as illustrated in Figure 4b, it appears that denitrification is the most probable pathway of the NO_3^- reduction. Similarly, low NO_3^- (0.6 mg L⁻¹) was recorded in MA4 during SW season, which was significantly low compared to other MA points. The dry periods (SW, D) appear to be favourable to denitrification mainly due to reduced water velocity which increases water residence time and contact with the river bed. Results of laboratory denitrification experiments on riverbed sediments demonstrate the relationship between NO_3^- loss (expressed as natural logarithm of the fraction of initial NO_3^- remaining in the sample) and increase in $\delta^{15}\text{N}$ (Figure 5). River Nyando sediment samples: MA4, MA5 showed NO_3^- decrease from 9.5 and 79 mg L⁻¹, respectively, at the start of the incubation to 0.1 and 2 mg L⁻¹ after 24 and 48 h of incubation, respectively. On the hand, $\delta^{15}\text{N}$ values increased from 13.7 (0 h) to 25.8 ‰ (8 h) for MA4 and from 6.5 (0 h) to 22.3 ‰ (30 h) for MA5 (Supplementary file: Table 4). The ¹⁵N enrichment factor due to denitrification, ϵ , is equal to the slope of the linear relationship between the natural logarithm of the fraction of NO_3^- remaining in a system and the change in $\delta^{15}\text{N}$ (Figure 5). The ¹⁵N enrichment factors obtained for the Nyando sediments were –17.5 and –17.2 ‰, respectively. These values are within the literature range (–3.0 to –29.4 ‰) of laboratory derived ¹⁵N enrichment factors for denitrification [25,40,41]. The sediment incubation results support the water chemistry and isotope observations (Figure 4b and c) to show that *in situ* denitrification is a potential process causing nitrate attenuation in River Nyando catchment. Consequently, the enrichment of $\delta^{15}\text{N}\text{-NO}_3^-$ due to denitrification may bias source apportionment, implying that manure/sewage may be overestimated.

3.2.3. Nzoia catchment

In the Nzoia catchment, a spatiotemporal variation in hydro-chemical parameters was observed as well (Figure 6a). Alkali metals were the dominant cations in U and MA land use stations while alkaline earth metals dominated CA. On the other hand, HCO_3^- dominance in CA and MA in the D season can be attributed to low water discharge levels (Table 1) which mainly consists of base flow solute levels while the $\text{Cl}^- + \text{NO}_3^-$ increase during PW season is associated with agricultural inputs (inorganic fertilizer, manure) during the wet cropping period. However, CA and MA exhibited similar anion concentration in the EW season which can be attributed to reduced application of inorganic/

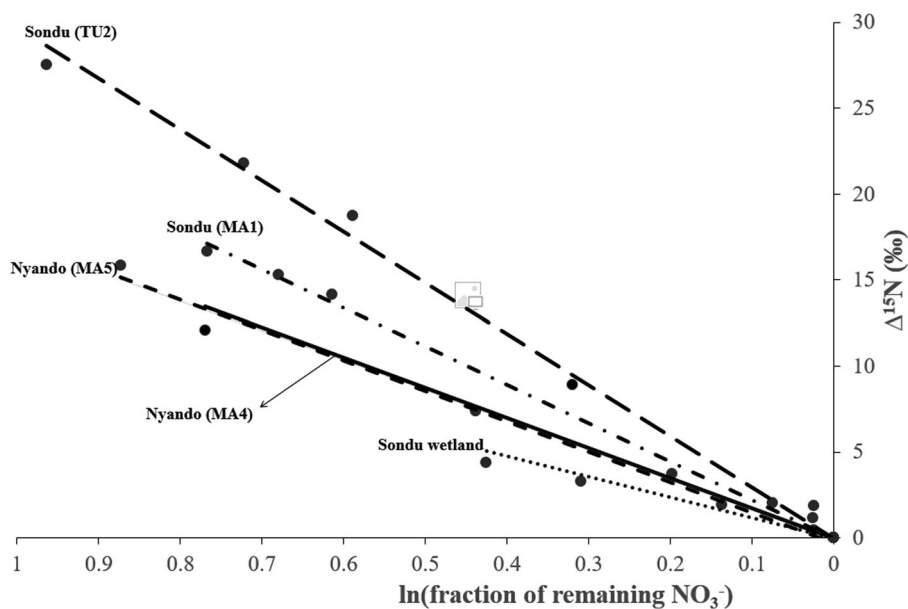


Figure 5. Determination of enrichment factors (ϵ , ‰) for potential denitrification in river bed sediments from Nyando and Sondu Miriu catchments. $\Delta^{15}\text{N} = \delta - \delta_0$, where δ represents $\delta^{15}\text{N}$ at time (t) and δ_0 represents initial $\delta^{15}\text{N}$. Denitrification enrichment factors: Nyando, MA4, $\epsilon = -17.5\text{‰}$; Nyando, MA5, $\epsilon = -17.2\text{‰}$; Sondu, TU2, $\epsilon = -29.7\text{‰}$; Sondu, MA1, $\epsilon = -22.3\text{‰}$; Sondu wetland, $\epsilon = -11.9\text{‰}$.

organic fertilizers because two out of the three main crops (maize and wheat) grown in the catchment are under harvest in this season while only sugarcane (perennial crop) remains in the farms. This is unlike observed in the Nyando catchment where tea and sugarcane (both perennial) are the main crops, and normally under fertilizer application in both PW and EW. U stations displayed $\text{Cl}^- + \text{NO}_3^-$ as the dominant anion in all seasons. Generally, the three land uses cluster around the centre of the diamond, portraying $\text{Ca} + \text{Mg} - \text{HCO}_3^-$, $\text{Na} + \text{K} - \text{HCO}_3^-$, $\text{Na} + \text{K} - \text{Cl} + \text{NO}_3^-$ and $\text{Ca} + \text{Mg} - \text{Cl} + \text{NO}_3^-$ water types. As earlier mentioned, $\text{Ca} + \text{Mg} - \text{HCO}_3^-$ represents soil weathering/natural solute sources while $\text{Na} + \text{K} - \text{Cl} + \text{NO}_3^-$, $\text{Ca} + \text{Mg} - \text{Cl} + \text{NO}_3^-$, and $\text{Na} + \text{K} - \text{HCO}_3^-$ water types indicates anthropogenic contamination [27,35] either of sewage or organic/inorganic fertilizer origin. This implies that sources of ionic constituents in the Nzoia catchment have similar contribution to the river mineralization. A Cl^- versus NO_3^- plot for the Nzoia catchment (Figure 6b) distinctly separates U (EW, D, SW) in a group having high Cl^- with corresponding lower NO_3^- concentration. However, U (PW) recorded relatively lower Cl^- concentrations, which can be attributed to dilution during the peak-wet season when the river exhibits high water discharge (Table 1). In addition, U stations had relatively high NH_4^+ levels ($1.9\text{--}2.5 \text{ mg L}^{-1}$) compared to CA and MA ($< 0.1 \text{ mg L}^{-1}$). The relatively high Cl^- and NH_4^+ concentrations observed in U imply sewage contamination from major urban centres such as Eldoret, a major industrial hub in western Kenya. Just as alluded in several studies [13,42,43] increase in population density and urbanization in Kenya, in the last two decades, has not been matched with the necessary planning and investment in sanitation infrastructure. This has led to the mushrooming of informal settlements ‘slums’ and industrial hubs which has outstretched

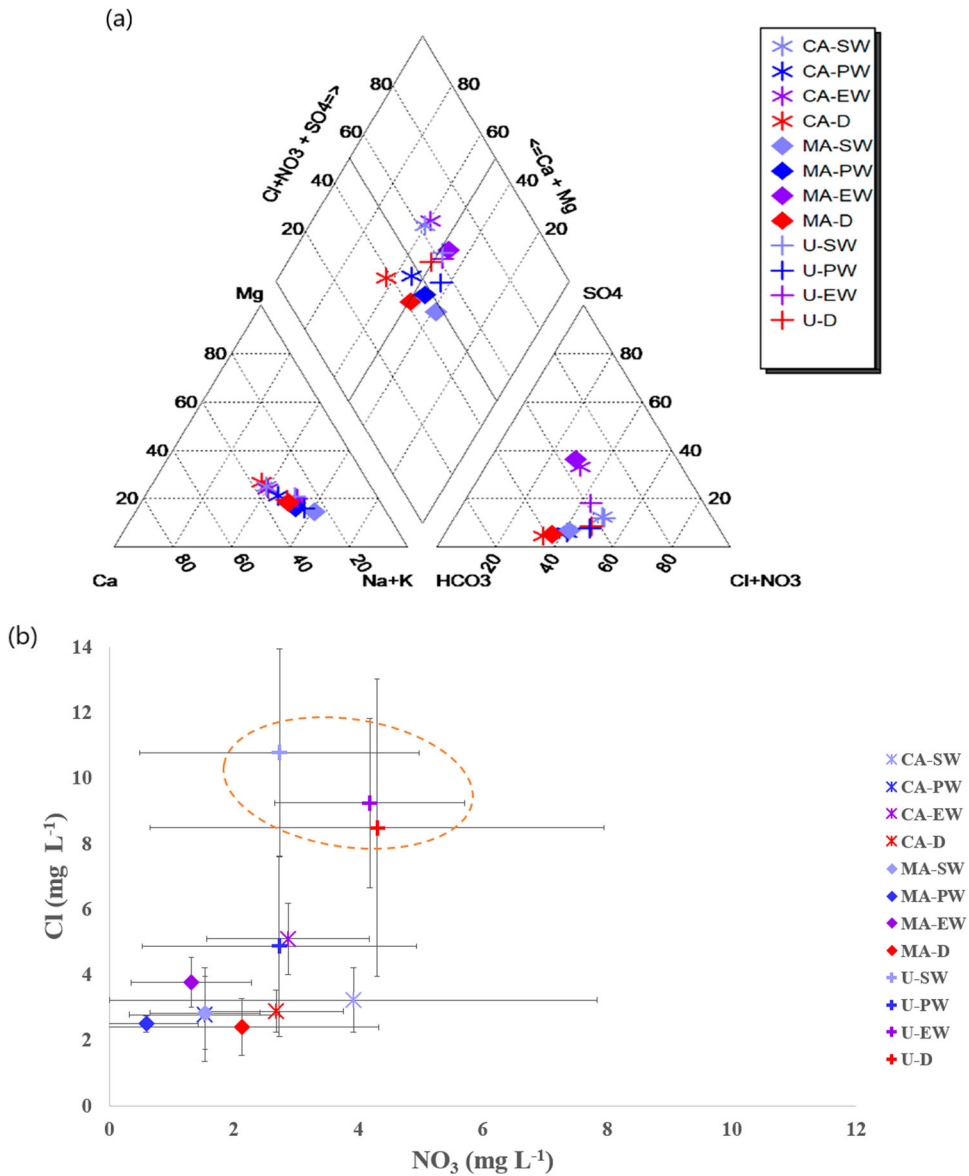


Figure 6. Nzoia catchment: Piper trilinear plot of major cations and anions (in percent) for water characterization. Bullets represent land use clusters (see Figure 3 for abbreviations), while colours represent selected sampling seasons (see Figure 2 for abbreviations) (a); spatial temporal plot of mean Cl^- versus NO_3^- mean concentrations with standard deviations given as error bars and bullets represent land use clusters while colours represent seasons as described in (a) above (b); Ranges of NO_3^- concentration, $\delta^{15}\text{N}-\text{NO}_3^-$ and $\delta^{18}\text{O}-\text{NO}_3^-$ values obtained for different land use clusters in Nzoia during start of wet (SW), peak wet (PW), end of wet (EW) and dry (D) seasons. Boxplots represent 25th, 50th, and 75th percentiles, whiskers represent 5th and 95th percentiles, black bullets represent outliers, and grey bullets represent mean values. Letters (a, b, c) represent ANOVA output with similar letters indicating non-significant difference ($p > 0.05$) using Tukey HSD test (c).

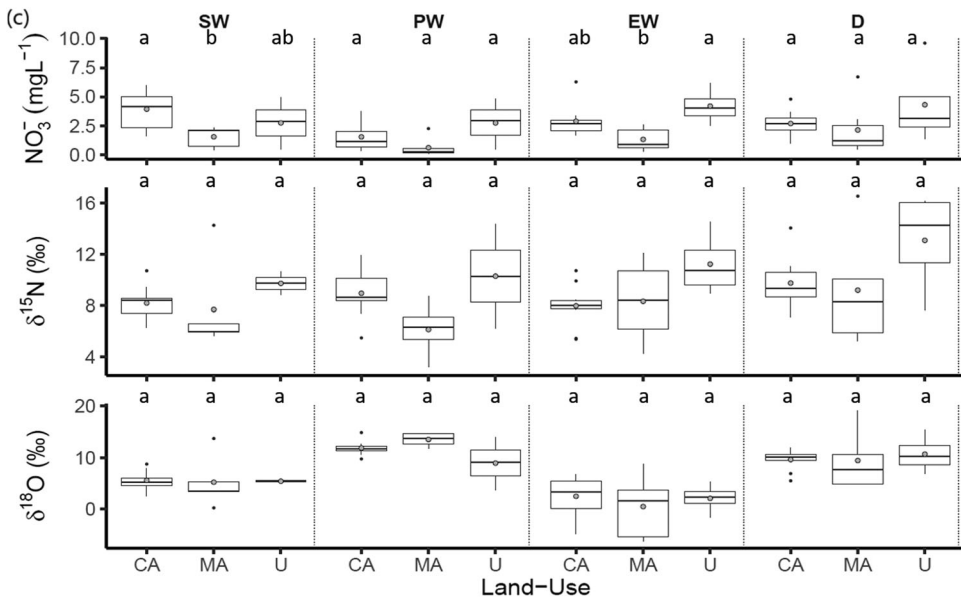


Figure 6 Continued

the existing sewage networks leading to discharge of raw or incompletely treated sewage into the rivers.

NO_3^- in the Nzoia catchment ranged from 0.1 mg L⁻¹ in MA during the PW season to maximum of 9.6 mg L⁻¹ in U during the dry season (Figure 6c). CA and U recorded higher NO_3^- concentration in the SW and EW seasons respectively, but similar NO_3^- concentration was observed across the catchment in the PW and D seasons. The $\delta^{15}\text{N}$ - NO_3^- values ranged from +3.2 to +16.5 ‰ showing no significant difference in the catchment. However, the relatively higher $\delta^{15}\text{N}$ - NO_3^- values obtained in U (PW and D seasons) confirm sewage as the main source of the river NO_3^- in agreement with hydrochemical findings (Figure 6b). $\delta^{18}\text{O}$ - NO_3^- values in the catchment are similar and generally lie in the nitrified N source range from -10 to +15 ‰ [2,44]. However, the relatively higher $\delta^{18}\text{O}$ - NO_3^- values obtained during the PW season in CA and MA suggest increased inorganic fertilizer contribution during the wet cropping season, an observation, which also agrees with hydrochemistry (Figure 6a).

3.2.4. Sondu Miriu catchment

In the Sondu Miriu catchment, alkali metals (Na^+ , K^+) dominated over the alkaline earth metals (Figure 7a), with Mg values below detection limit during the wet seasons (PW, EW). On the other hand, $\text{Cl}^- + \text{NO}_3^-$ were the dominant anions, therefore, giving $\text{Na} + \text{K} + \text{Cl} + \text{NO}_3^-$ as the main water type in the Sondu Miriu catchment. An increase in $\text{Cl}^- + \text{NO}_3^-$ concentration was observed during PW season across the land uses with TU giving the highest $\text{Cl}^- + \text{NO}_3^-$ levels, an indicator of increased inorganic fertilizer contribution during the wet season and especially in the commercial tea farms. Given the main land use in this catchment was tea farming, it implies that the ammonium based inorganic fertilizer (NPK, 25:5:5 + 5S) which is the most commonly applied in tea farming contributes

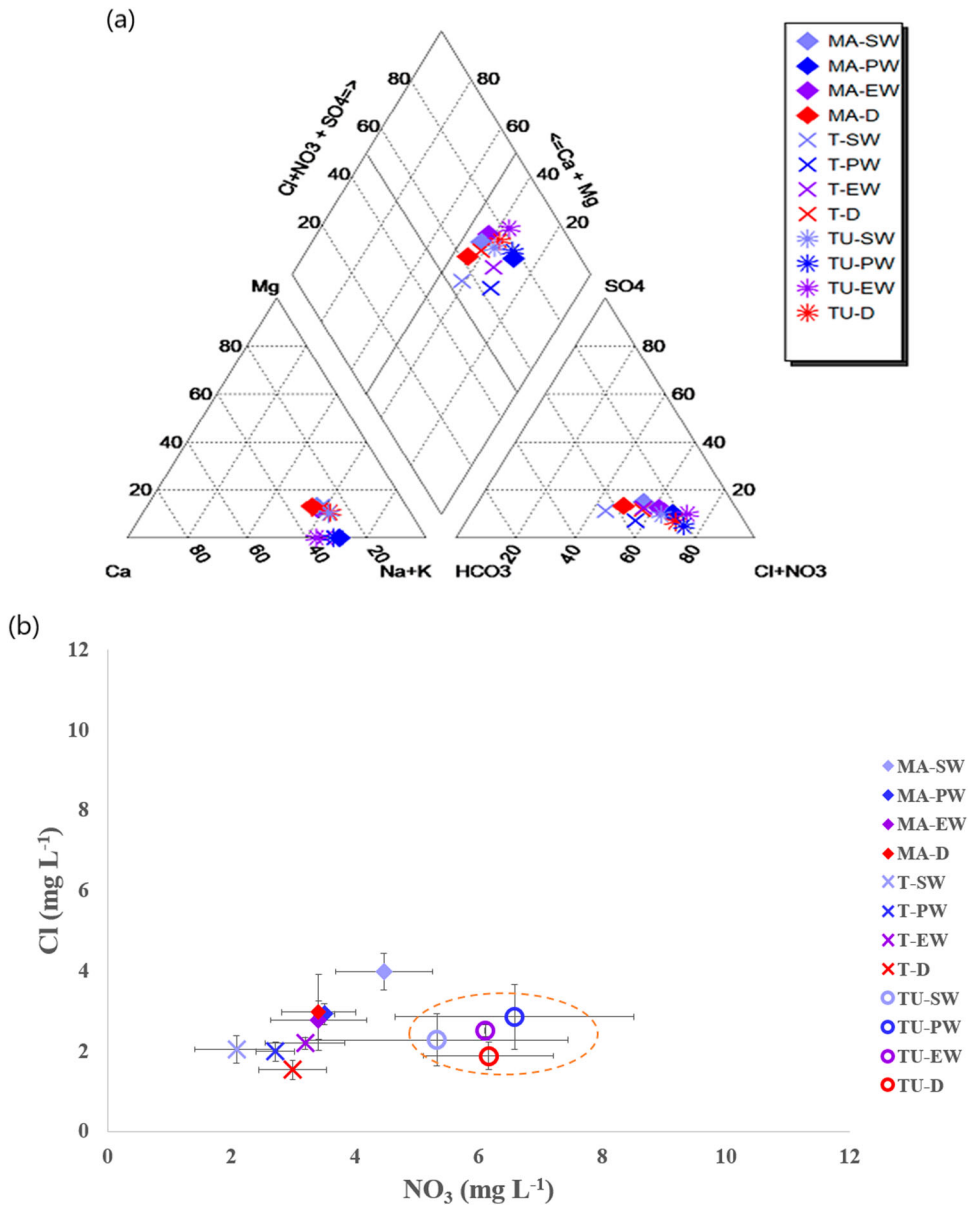


Figure 7. Sondu Miriu catchment: Piper trilinear plot of major cations and anions (in percent) for water characterization. Bullets represent land use clusters (see Figure 3 for abbreviations), while colours represent selected sampling seasons (see Figure 2 for abbreviations) (a); spatial temporal plot of mean Cl versus NO₃ mean concentrations with standard deviations given as error bars and bullets represent land use clusters while colours represent seasons as described in (a) above (b); Ranges of NO₃ concentration, δ¹⁵N–NO₃ and δ¹⁸O–NO₃ values obtained for different land use clusters in Sondu Miriu during start of wet (SW), peak wet (PW), end of wet (EW) and dry (D) seasons. Boxplots represent 25th, 50th, and 75th percentiles, whiskers represent 5th and 95th percentiles, black bullets represent outliers, and grey bullets represent mean values. Letters (a, b, c) represent ANOVA output with similar letters indicating non-significant difference ($p > 0.05$) using Tukey HSD test(c).

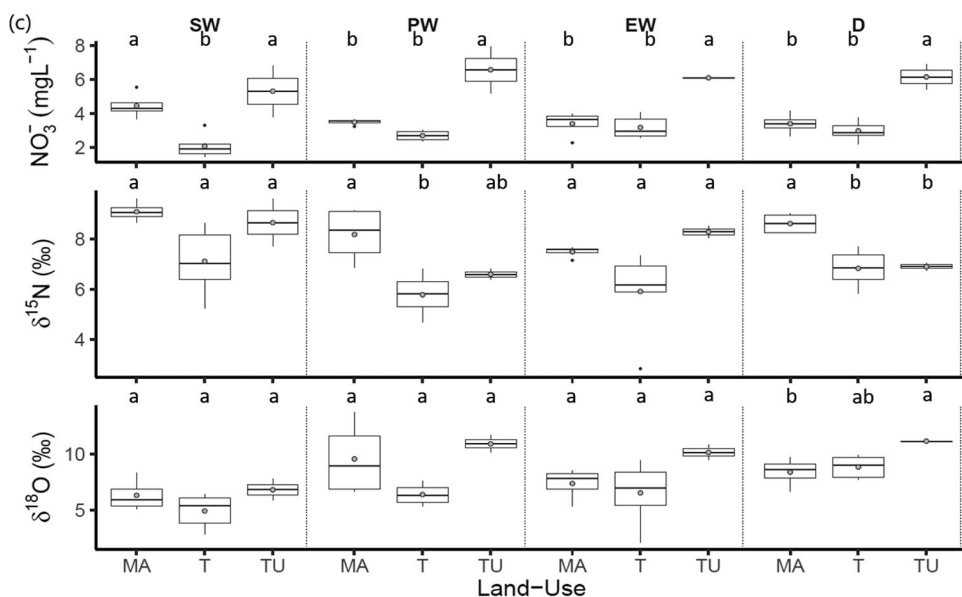


Figure 7 Continued

significantly to the Na + K-Cl + NO₃ water type, and has a higher influence during the wet seasons. The Cl⁻ versus NO₃⁻ plot (Figure 7b) of the Sondu Miriu catchment clearly separates TU in a group with high NO₃⁻ content without matching high Cl⁻ concentration. TU land use consisted of a zone covering approximately 20,000 ha under commercial tea plantation, which practiced aerial fertilizer application with an annual application rate of 38–63 kg N ha⁻¹ [45]. Hence, the relatively high NO₃⁻ levels corresponding to low Cl⁻ concentration observed in TU was due to the ammonium based NPK fertilizer type (25:5:5 + 5S) used whose potassium (K) form is K(SO₄)₂ and not potash (KCl).

NO₃⁻ in the Sondu Miriu catchment ranged from a minimum of 1.5 mg L⁻¹ in T during the SW season to a maximum of 8.0 mg L⁻¹ (Figure 7c) in TU during the PW season. TU recorded generally higher NO₃⁻ levels in all seasons, while MA and T had similar concentrations in all but the SW season when T recorded the lowest concentration. This can be attributed to the higher rate of inorganic fertilizer application in the commercial tea estates of the TU (38–63 kg N ha⁻¹) compared to the small scale tea farms of the T land use (13–30 kg N ha⁻¹), and mixed farms (MA) where animal manure is commonly applied [45]. On the other hand, δ¹⁵N–NO₃⁻ values in the Sondu Miriu catchment ranged from +2.8 in T to +9.6 ‰ in TU with MA giving significantly higher mean δ¹⁵N–NO₃⁻ values during the PW and D seasons. The δ¹⁸O–NO₃⁻ values ranged from +2.2 in T to +13.7 ‰ in MA. δ¹⁸O–NO₃⁻ values in Sondu Miriu catchment were similar in all seasons except during the D season when TU gave significantly high values. Given that MA land use of this catchment is characterized by rural residences purely lacking conventional sanitation infrastructure and free ranch livestock keeping, the higher δ¹⁵N–NO₃⁻ values obtained during PW and D seasons (mean: +8.2 and 8.7 ‰, respectively) reveal increased river NO₃⁻ input from animal manure and domestic sewage sources. The high NO₃⁻ concentration reported in TU in all seasons supports hydrochemical observations (Figure 7b) that

the ammonium-based fertilizer 'NPK' commonly used in the commercial tea estates dominates river NO_3^- input. The Sondu Miriu catchment generally portray a Na + K-Cl + NO_3^- water type and lower $\delta^{15}\text{N}-\text{NO}_3^-$ values (relative to Nyando and Nzoia), implying that inorganic fertilizers are more dominating sources of river NO_3^- in the catchment. This agrees with Jacobs et al [45] who observed that land use strongly affects river NO_3^- in the Sondu Miriu River catchment. The authors also observed that river NO_3^- in land use areas, dominated by commercial tea plantations had higher NO_3^- concentrations than natural forest areas.

Denitrification enrichment factors, ϵ , obtained from laboratory incubation of Sondu Miriu river sediments (Figure 5) were -11.9 (wetland), -22.3 (MA1), and -29.7 ‰ (TU2). These values are within the range of laboratory derived ^{15}N enrichment factors for denitrification reported by Wells et al [41]. However, possible reason for variability in enrichment factors for denitrification amongst the sediments is difference in temperature or the organic carbon (electron donor) to nitrate (electron acceptor) ratio [25,41]. Denitrification rate is assumed to have controlling influence on the enrichment factor, and also denitrification is a first order reaction where low rates (caused by low quantity of electron donor) result into larger fractionations while high rates (high temperatures or high electron donor content) result into smaller fractionations [46]. For the current study, there was no temperature variation in the experiment (room temperature: 20°C), therefore, lower fractionations observed in the wetland sample is due to its higher carbon/nitrate ratio (Supplementary file: Table 4). It is therefore likely that, denitrification is contributing to the relatively lower NO_3^- and enriched isotope values obtained in these sections of the Sondu Miriu catchment. However, NO_3^- uptake by wetland vegetation [25,47] is the other potential NO_3^- reduction mechanism taking place in the study area.

Although river NO_3^- data in the Lake Victoria (Kenya) basin are limited, NO_3^- levels obtained in this study are higher than those available in literature for Kenyan river catchments in the basin: $1.3\text{--}7.2$ mg L^{-1} [45], $0.16\text{--}0.38$ mg L^{-1} [36], 5.3 ± 1.3 mg L^{-1} [48], and $0.8\text{--}1.0$ mg L^{-1} [34]. Therefore, a clear indication of increasing NO_3^- concentration and discharge into Lake Victoria appears, which confirms the significant contribution of river catchments to the eutrophic conditions prevailing in the lake. From findings of this study, it is evident that increasing river NO_3^- concentration in the basin is driven largely by inorganic fertilizer losses from commercial agriculture, manure losses from mixed agriculture, and untreated sewage effluent (domestic and urban) discharges.

4. Conclusions and recommendations

Physico-chemical data of water from major river catchments in the Lake Victoria basin, Kenya, allowed clear separation and clustering of river water sampling stations corresponding to major land use classes of the catchments. The NO_3^- levels observed in this study are higher than those reported in preceding studies, indicating increasing NO_3^- concentrations in surface waters of the basin. In addition, our findings show that sources of NO_3^- and solute discharge in the river catchments vary with land use and seasons. Inorganic fertilizers and soil N are the main sources of riverine NO_3^- input in the predominantly tea growing land uses of the Sondu Miriu and Nyando river catchments, while both sewage and inorganic/organic fertilizers dominate in the mixed agriculture areas of the three catchments. The more urbanized areas (U, RI) displayed sewage as the dominant

source of river NO_3^- input. Seasonally, inorganic/organic fertilizer losses dominate river NO_3^- input during the wet cropping season in the three catchments. However, laboratory derived ^{15}N enrichment factors for riverbed sediments are consistent with a potential active denitrification process. Such process could explain significantly low NO_3^- concentrations observed in the S and RI land use areas of the Nyando catchment (SW, D seasons) together with the relatively lower NO_3^- levels reported in the Sondu Miriu catchment, but at the same time bias source apportionment. It is recommended that a future sampling and water quality-monitoring network in the basin should be designed to capture the major land use patterns: sugarcane, tea, mixed agriculture, residential/industrial, urban and forests. A land-use based monitoring network will not only reduce the number of sampling stations and field costs. It also simplifies pollution control measures by focusing mitigating efforts on specific pollution impacts from each land use activity. To mitigate the increasing NO_3^- concentration trend, sewage and effluent collection and treatment facilities should be upgraded and extended to cover all urban, residential, and agricultural areas. In addition, soil fertility levels and other precision agricultural practices should be established in the basin in order to develop optimum fertilizer application rates for maximizing crop yields while at the same time minimizing nutrient losses into the rivers.

Acknowledgements

We acknowledge the contribution of David Haaf (ETH Zurich) in developing Land use maps and the Ministry of Water & Irrigation-Kenya for human resource and field facilitation support.

Disclosure statement

No potential conflict of interest was reported by the authors.

Funding

This study was funded through a VLIRUOS (Belgium) TEAM project 'Improved management for nitrate pollution in the Lake Victoria catchment of Kenya - ZEIN2016PR423'.

ORCID

Benjamin Nyalitya  <http://orcid.org/0000-0002-2796-1886>

Pascal Boeckx  <http://orcid.org/0000-0003-3998-0010>

References

- [1] Sacchi E, Acutis M, Bartoli M, et al. Origin and fate of nitrates in groundwater from the central Po plain: Insights from isotopic investigations. *Appl Geochemistry*. 2013;34:164–180.
- [2] Kendall C, Elliott EM, Wankel SD. Tracing anthropogenic inputs of nitrogen to ecosystems. In: Michener R, Lajtha K, editor. *Stable isotopes in ecology and environmental science*, 2nd ed. Oxford, UK: Blackwell Publishing Ltd.; 2007. p. 375–449.
- [3] Schullehner J, Hansen B, Thygesen M, et al. Nitrate in drinking water and colorectal cancer risk: A nationwide population-based cohort study. *Int J Cancer*. 2018;143(1):73–79.

- [4] Benkovitz CM, Scholtz MT, Pacyna J, et al. Global gridded inventories of anthropogenic emissions of sulfur and nitrogen. *J Geophys Res Atmos.* **1996**;101(D22):29239–29253.
- [5] Sitoki L, Gichuki J, Ezekiel C, et al. The environment of Lake Victoria (East Africa): current status and historical changes. *Int Rev Hydrobiol.* **2010**;95(3):209–223.
- [6] Talling JF, Talling IB. The chemical composition of African lake waters. *Int Rev Ges Hydrobiol.* **1965**;50:421–463.
- [7] Gophen M, Ochumba P, Kaufman L. Some aspects of perturbation in the structure and biodiversity of the ecosystem of Lake Victoria (East Africa). *Aquat Living Resour.* **1995**;8:27–41.
- [8] Lung'ayia H, Sitoki L, Kenya M. The nutrient enrichment of Lake Victoria (Kenyan waters). *Hydrobiologia.* **2001**;458:75–82.
- [9] Gikuma-Njuru P, Hecky RE. Nutrient concentrations in Nyanza Gulf, Lake Victoria, Kenya: Light limits algal demand and abundance. *Hydrobiologia.* **2005**;534(1–3):131–140.
- [10] Gikuma-Njuru P, Hecky RE, Guildford SJ, et al. Spatial variability of nutrient concentrations, fluxes, and ecosystem metabolism in Nyanza Gulf and Rusinga Channel, Lake Uictoria (East Africa). *Limnol Oceanogr.* **2013**;58(3):774–789.
- [11] UNEP, WHRC. Reactive Nitrogen in the Environment: Too Much or too Little of a Good Thing. Paris: United Nations Environ Program;1–56; 2007.
- [12] COWI consulting engineers. Integrated Water Quality / Limnology Study for Lake Victoria. Lake Victoria Environmental Management Project, Part II Technical Report. 2002;(March).
- [13] Juma DW, Wang H, Li F. Impacts of population growth and economic development on water quality of a lake: Case study of Lake Victoria Kenya water. *Environ Sci Pollut Res.* **2014**;21(8):5737–5746.
- [14] ICRAF. Global Environment Facility. Project proposal for a Full Sized Project. Nairobi, Kenya; 2003.
- [15] Zhou M, Brandt P, Pelster D, et al. Regional nitrogen budget of the Lake Victoria Basin, East Africa: Syntheses, uncertainties and perspectives. *Environ Res Lett.* **2014**;9(10):105009.
- [16] Nyenje PM, Foppen JW, Uhlenbrook S, et al. Eutrophication and nutrient release in urban areas of sub-Saharan Africa - A review. *Sci Total Environ.* **2010**;408(3):447–455.
- [17] Kansiime F, Kateyo E, Oryem-Origa H, et al. Nutrient status and retention in pristine and disturbed wetlands in Uganda: management implications. *Wetl Ecol Manag.* **2007**;15(6):453–467.
- [18] Xue D, Botte J, De Baets B, et al. Present limitations and future prospects of stable isotope methods for nitrate source identification in surface- and groundwater. *Water Res.* **2009**;43:1159–1170.
- [19] Zeng H, Wu J. Tracing the nitrate sources of the Yili River in the Taihu Lake watershed: A dual isotope approach. *Water (Switzerland).* **2015**;7(1):188–201.
- [20] Panno S, Hackley K, Kelly W, et al. Isotopic evidence of nitrate sources and denitrification in the Mississippi River, Illinois. *J Environ Qual.* **2006**;35:495–504.
- [21] Mayer B, Van Breemen N, Howarth RW, et al. Sources of nitrate in rivers draining sixteen watersheds in the northeastern U.S.: isotopic constraints. *Biogeochemistry.* **2002**;57–58:171–197.
- [22] Team CW, Pachauri R, Reisinger AA. Contribution of working groups I,II and III to the fourth assesment report of the Intergovernmental Panel On Climate Change, IPCC. Geneva: Intergovernmental Panel on Climate Change; **2007**; 546.
- [23] Casciotti KL, Sigman DM, Hastings MG, et al. Measurement of the oxygen isotopic composition of nitrate in seawater and freshwater using the denitrifier method. *Anal Chem.* **2002**;74(19):4905–4912.
- [24] Sigman DM, Casciotti KL, Andreani M, et al. A bacterial method for the nitrogen isotopic analysis of nitrate in seawater and freshwater. *Anal Chem.* **2001**;73(17):4145–4153.
- [25] Dhondt K, Boeckx P, Van Cleemput O, et al. Quantifying nitrate retention processes in a riparian buffer zone using the natural abundance of ¹⁵N in NO₃⁻. *Rapid Commun Mass Spectrom.* **2003**;17(23):2597–2604.
- [26] Barakat A, El Baghdadi M, Rais J, et al. Assessment of spatial and seasonal water quality variation of Oum Er Rbia River (Morocco) using multivariate statistical techniques. *Int Soil Water Conserv Res.* **2016**;4(4):284–292.

- [27] Kamtchueng BT, Fantong WY, Wirmvem MJ, et al. Hydrogeochemistry and quality of surface water and groundwater in the vicinity of Lake Monoun, West Cameroon: approach from multivariate statistical analysis and stable isotopic characterization. *Environ Monit Assess.* 2016;188(9):524.
- [28] Pejman AH, Nabi Bidhendi GR, Karbassi AR, et al. Evaluation of spatial and seasonal variations in surface water quality using multivariate statistical techniques. *Int J Environ Sci Technol.* 2009;6(3):467–476.
- [29] Zhang Q, Li Z, Zeng G, et al. Assessment of surface water quality using multivariate statistical techniques in red soil hilly region: A case study of Xiangjiang watershed, China. *Environ Monit Assess.* 2009;152(1–4):123–131.
- [30] Piper A. A graphical procedure in the geochemical interpretation of water analysis. *Trans Am Geophys Union.* 1944;25:914–923.
- [31] Widory D, Petelet-Giraud E, Négrel P, et al. Tracking the sources of nitrate in groundwater using coupled nitrogen and boron isotopes: A synthesis. *Environ Sci Technol.* 2005;39(2):539–548.
- [32] Nestler A, Berglund M, Accoe F, et al. Isotopes for improved management of nitrate pollution in aqueous resources: Review of surface water field studies. *Environ Sci Pollut Res.* 2011;18(4):519–533.
- [33] Piña-Ochoa E, Álvarez-Cobelas M. Denitrification in aquatic environments: A cross-system analysis. *Biogeochemistry.* 2006;81(1):111–130.
- [34] Okungu J, Opango P. Pollution loads into Lake Victoria from the Kenyan catchment. 2004 [cited 2018 Sep 9]. Available from: http://www.lvemp.org/L_Publications/kenya/Okunguj.pdf.
- [35] Ako AA, Shimada J, Hosono T, et al. Spring water quality and usability in the Mount Cameroon area revealed by hydrogeochemistry. *Environ Geochem Health.* 2012;34(5):615–639.
- [36] Nyairo WN, Owuor PO, Kengara FO. Effect of anthropogenic activities on the water quality of Amala and Nyangores tributaries of River Mara in Kenya. *Environ Monit Assess.* 2015;187(11):691.
- [37] Liu C, Li S, Lang Y, et al. Using $\delta^{15}\text{N}$ - and $\delta^{18}\text{O}$ -values to identify nitrate sources in Karst Ground Water, Guiyang, Southwest China. *Environ Sci Technol.* 2006;40(22):6928–6933.
- [38] Mengis M, Schill S, Harris M, et al. Multiple geochemical and isotopic approaches for assessing groundwater nitrate elimination in a riparian zone. *Groundwater.* 1999;37(3):448–457.
- [39] Hill AR. Nitrate removal in stream riparian zones. *J Environ Qual.* 1996;25:743–755.
- [40] Blackmer A, Bremner J. Nitrogen isotope discrimination in denitrification of nitrate in soils. *Soil Biol Biochem.* 1977;9:73–77.
- [41] Wells NS, Clough TJ, Johnson-Beebout SE, et al. Effects of denitrification and transport on the isotopic composition of nitrate ($\delta^{18}\text{O}$, $\delta^{15}\text{N}$) in freshwater systems. *Sci Total Environ.* 2019;651:2228–2234.
- [42] Wang H, Wang T, Toure B, et al. Protect lake Victoria through green economy, public participation and good governance. *Environ Sci Technol.* 2012;46(19):10483–4.
- [43] Marwick TR, Tamooh F, Ogwoka B, et al. Dynamic seasonal nitrogen cycling in response to anthropogenic N loading in a tropical catchment, Athi-Galana-Sabaki River, Kenya. *Biogeosciences.* 2014;11(2):443–460.
- [44] Mayer B, Bollwerk SM, Mansfeldt T, et al. The oxygen isotope composition of nitrate generated by nitrification in acid forest floors. *Geochim Cosmochim Acta.* 2001;65(16):2743–2756.
- [45] Jacobs SR, Breuer L, Butterbach-Bahl K, et al. Land use affects total dissolved nitrogen and nitrate concentrations in tropical montane streams in Kenya. *Sci Total Environ.* 2017;603–604:519–532.
- [46] Mariotti A, Germon J, Leclerc A. Nitrogen isotope fractionation associated with the NO_2 - N_2O step of denitrification in soils. *Can Journal Soil Sci.* 1982;62:227–241.
- [47] Lund LJ, Horne AJ, Williams AE. Estimating denitrification in a large constructed wetland using stable nitrogen isotope ratios. *Ecol Eng.* 1999;14(1–2):67–76.
- [48] Kipkemboi J, McClain ME, Gettel GM, et al. Litter processing and shredder distribution as indicators of riparian and catchment influences on ecological health of tropical streams. *Ecol Indic.* 2014;46:23–37.